Hepatocarcinogenesis: Multistep Changes of Drainage Vessels at CT during Arterial Portography and Hepatic Arteriography—Radiologic-Pathologic Correlation[1]

Azusa Kitao, MD
Yoh Zen, MD
Osamu Matsui, MD
Toshifumi Gabata, MD
Yasuni Nakanuma, MD

Purpose: To clarify the changes that occur in drainage vessels of dysplastic nodules and hepatocellular carcinoma (HCC) during hepatocarcinogenesis by using computed tomography (CT) during arterial portography (CTAP) and CT during hepatic arteriography (CTHA), with histologic findings as the reference standard.

Materials and Methods: Institutional ethics committee approval and informed consent were obtained. According to the findings at CTAP and CTHA, 46 surgically resected hepatocellular nodules were classified into three types: type A (n = 18) (equivalent or decreased portal perfusion compared with background liver at CTAP, decreased arterial perfusion, and no corona enhancement [perinodular contrast material drainage] at CTHA), type B (n = 13) (no portal perfusion, increased arterial perfusion, and thin (≤2-mm) corona enhancement), or type C (n = 15) (no portal perfusion, increased arterial perfusion, and thick (>2-mm) corona enhancement). We compared the histopathologic features and microangioarchitecture between the types.

Results: Type A nodules histologically consisted of dysplastic nodules and well-differentiated HCC; type B and C nodules were moderately differentiated HCC. Replacing growth was commonly observed in type A nodules, whereas compressing growth was more frequently seen in types B and C. Sixty percent of type C nodules had a fibrous capsule. There were significantly fewer intranodular hepatic veins in types B and C. Serial pathologic slices demonstrated continuity from intranodular capillarized sinusoids to hepatic veins in type A nodules and to surrounding hepatic sinusoids in type B nodules. In type C nodules, intranodular capillarized sinusoids were connected to extranodular portal veins either directly or through portal venules within the fibrous capsule.

Conclusion: Drainage vessels of HCC change from hepatic veins to hepatic sinusoids and then to portal veins during multistep hepatocarcinogenesis.

[1] From the Departments of Radiology (A.K., O.M., T.G.) and Human Pathology (A.K., Y.Z., Y.N.), Kanazawa University Graduate School of Medical Science, 13-1 Takaramachi, Kanazawa 920-8640, Japan. Received August 10, 2008; revision requested September 24; revision received January 7, 2009; accepted March 2; final version accepted March 16. Supported in part by Grant-in-Aid for Cancer Research (no. 18S-01) from Ministry of Health, Labor, and Welfare and by Health and Labor Sciences Research Grants for Development of Novel Molecular Markers and Imaging Modalities for Earlier Diagnosis of Hepatocellular Carcinoma. **Address correspondence to** A.K. (e-mail: *kitao@rad.m.kanazawa-u.ac.jp*).

Hepatocellular carcinoma (HCC) is usually associated with chronic liver disease, especially chronic viral hepatitis and liver cirrhosis (1,2). HCC has been proved to develop by multistep carcinogenesis from a dysplastic nodule (DN), to early HCC (highly well-differentiated HCC), and finally to overt hypervascular HCC (moderately differentiated HCC) (3–10).

To understand the pathophysiology of HCC, especially in its early stage, the multistep changes in the blood supply of DNs and HCC have been well studied with radiologic techniques (11,12). Computed tomography (CT) during arterial portography (CTAP) and CT during hepatic arteriography (CTHA) are useful radiologic methods for evaluating in vivo dynamics of portal supply and arterial supply, respectively, in hepatic lesions (11–17). DNs show the same or mildly decreased portal perfusion at CTAP and decreased arterial perfusion at CTHA compared with surrounding liver parenchyma. On the other hand, moderately differentiated HCC shows no portal perfusion at CTAP and clearly increased arterial perfusion at CTHA. In brief, the inflow of nodules changes from a mainly portal supply to an exclusively arterial supply during the multistep hepatocarcinogenesis (12). These radiologic findings reflect the histologic vascular structure of HCC (18,19).

Advances in Knowledge

- The main drainage vessels of hepatocellular carcinoma (HCC) change from hepatic veins to hepatic sinusoids to portal veins during multistep hepatocarcinogenesis.
- The thickness of corona enhancement (perinodular drainage of contrast material) of HCC at late-phase CT during hepatic arteriography correlates with the histologic grade of tumor malignancy and the type of drainage vessels.
- The changes in HCC drainage vessels could be triggered by the early reduction of intranodular hepatic veins owing to tumor invasion.

In comparison to inflow, little attention has been paid to drainage flow of HCC and DNs, although a few radiologic studies regarding drainage vessels of HCC have been published (20–22). Ueda et al (22) used single-level dynamic CTHA to clarify the drainage vessels of hypervascular HCC with a fibrous capsule. In their study, intranodular contrast enhancement was observed, and subsequently, perinodular enhancement with bright branching structures appeared on single-level dynamic CTHA images. They concluded that perinodular enhancement, named *corona enhancement*, is the drainage area of the tumor and that the branching structures are portal venules corresponding to the drainage route. However, the radiologic-pathologic correlation has not been fully elucidated. In particular, how the drainage vessels change during multistep hepatocarcinogenesis has not been examined.

In our study, we tried to clarify the changes that occur in drainage vessels during hepatocarcinogenesis from DN to moderately differentiated HCC. We evaluated intranodular and perinodular hemodynamics by using CTAP and CTHA, with a focus on the correlation of corona enhancement at late-phase CTHA with histopathologic features.

Materials and Methods

Patients

This retrospective study was performed with the approval of the institutional ethics committee, and informed consent was obtained from patients. It focused on 46 hepatocellular nodules in 40 patients, which were surgically resected and were pathologically diagnosed as DNs or HCC at our institution between 1998 and 2007. We did not include large (>6 cm in diameter) nodules or poorly differentiated HCCs, because they are often associated with secondary changes that might influence imaging (eg, necrosis, hemorrhage, invasion of the portal or hepatic veins). All patients (mean age, 61.0 years ± 8.4 [standard deviation]; men, 85%; women, 15%) had chronic liver disease. No patient had previously undergone treatment (eg, ablation therapy, transarterial chemoembolization therapy, chemotherapy) for hepatocellular nodules.

Implications for Patient Care

- The grade of tumor malignancy may be indicated by analyzing corona enhancement of HCC at dynamic CT, dynamic MR imaging, or contrast-enhanced US.
- Knowledge of venous drainage is important for understanding the pathophysiology of HCC and for precise performance of interventional therapy or surgical resection.

CTAP and CTHA

Both CTAP and CTHA were performed in all patients before surgical resection (mean time before surgery, 41.3 days ± 17.8) because of their extremely high sensitivity for detection of other nodular lesions (11). CTAP and CTHA were performed with various CT scanners (XVision SP, Toshiba Medical Systems, Tokyo, Japan; Aquilion 64, Toshiba Medical Systems; HiSpeed Advantage, GE Healthcare, Milwaukee, Wis; and LightSpeed Ultra 16, GE Healthcare). From the femoral artery, 4-F catheters were inserted into the superior mesenteric artery for CTAP and into

Published online
10.1148/radiol.2522081414

Radiology 2009; 252:605–614

Abbreviations:
CTAP = CT during arterial portography
CTHA = CT during hepatic arteriography
DN = dysplastic nodule
HCC = hepatocellular carcinoma

Author contributions:
Guarantors of integrity of entire study, all authors; study concepts/study design or data acquisition or data analysis/interpretation, all authors; manuscript drafting or manuscript revision for important intellectual content, all authors; approval of final version of submitted manuscript, all authors; literature research, A.K., O.M.; clinical studies, A.K., Y.Z., O.M., T.G., Y.N.; statistical analysis, A.K.; and manuscript editing, A.K., Y.Z., O.M., Y.N.

Authors stated no financial relationship to disclose.

the common, proper, or replaced right hepatic artery for CTHA.

CTAP scans were obtained at 5–7-mm section thickness and 5–7-mm collimation to cover the entire liver in a single breath hold. To increase the blood flow and decrease the laminar flow of the portal vein, 5 μg of prostaglandin E1 (Palux; Taisho, Tokyo, Japan) was injected into the superior mesenteric artery before contrast material infusion. Helical scanning began 25 seconds after the infusion of 50–70 mL of iohexol (320–350 milligrams of iodine per milliliter) (Omnipaque; Daiichi, Tokyo, Japan) at a rate of 1.8 mL/sec by using a power injector was started.

CTHA scans were obtained at 3–5-mm section thickness and 3–5-mm collimation. Helical scanning was started 7 seconds after the beginning of an infusion of iohexol (320–350 milligrams of iodine per milliliter) into the common, proper, or replaced hepatic artery at a rate of 1.8 mL/sec. The infusion of contrast material was continued until 5 seconds after early-phase CTHA scanning was completed. The scanning time varied according to the individual liver size (about 20–25 seconds). The total amount of contrast medium varied according to the following equation: (early-phase scanning time + 12 seconds) × injection rate. Thirty seconds after contrast material infusion finished (about 62–67 seconds after the infusion began), late-phase scanning commenced.

Radiologic Classification of Hepatocellular Nodules

The nodules were retrospectively classified into three types according to the findings at CTAP and CTHA in consensus by two radiologists (A.K. and O.M., with 8 and 38 years experience, respectively) who were blinded to any pathologic information. The classifications were determined on the basis of past reports about the findings of CTAP and CTHA.

We defined a type A nodule as a nodular lesion that showed equivalent or decreased portal perfusion as compared with background liver on CTAP images, decreased arterial perfusion compared with background liver on early-phase CTHA images, and no perinodular stain-

Figure 1

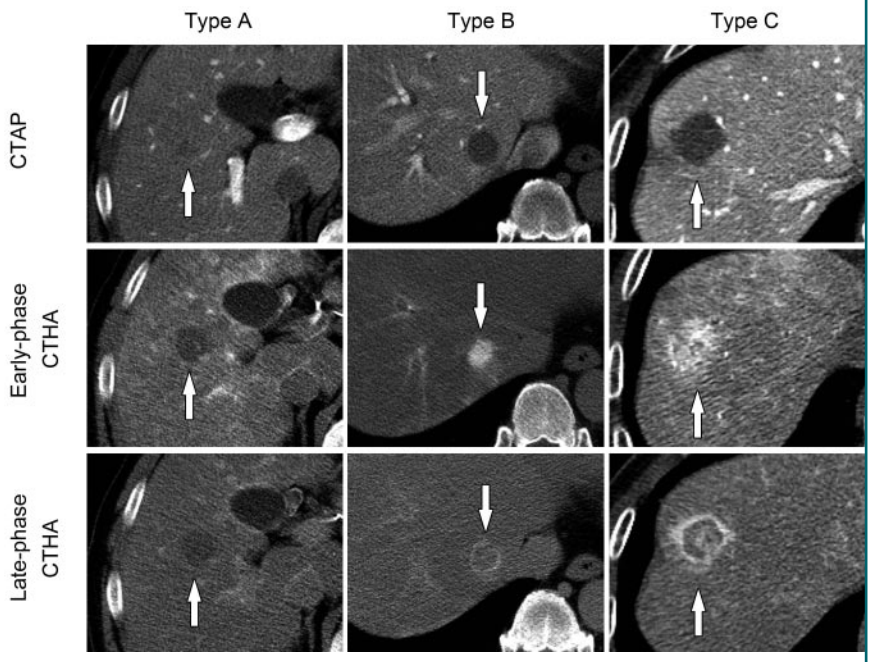

Figure 1: Typical CTAP (top row), early-phase CTHA (middle row), and late-phase CTHA (bottom row) findings for the three nodule types (arrows). Type A nodule (left column) has equivalent-to-decreased portal perfusion on CTAP imaging, decreased arterial perfusion on early-phase CTHA images, and no corona enhancement on late-phase CTHA images. Type B nodule (middle column) has portal perfusion defect and increased arterial perfusion with thin corona enhancement. Type C nodule (right column) has portal perfusion defect, increased arterial perfusion, and thicker corona enhancement.

Clinical Features by Tumor Type

Clinical Feature	Type A	Type B	Type C
No. of tumors	18	13	15
Resected tumor size (cm)*	2.0 ± 1.2 (0.9–4.8)	2.7 ± 1.6 (1.2–5.2)	2.6 ± 1.2 (1.6–5.5)
Age (y)*	58.9 ± 6.6 (47–70)	62.6 ± 8.9 (53–71)	62.7 ± 9.6 (53–76)
Male-to-female ratio	14:4	10:3	14:1
Underlying disease process			
Chronic hepatitis	6	3	6
Hepatitis B virus	2	0	1
Hepatitis C virus	4	3	4
Hepatitis B and C viruses	0	0	1
Liver cirrhosis	12	10	9
Hepatitis B virus	3	4	5
Hepatitis C virus	7	5	3
Cryptogenic	2	1	1

Note.—Unless otherwise specified, data are numbers of patients.

* Data are means ± standard deviations, with ranges in parentheses.

ing corona enhancement on late-phase CTHA images. Type B nodules showed no portal perfusion, clearly increased arterial perfusion compared with background liver, and thin corona enhancement. Thin corona enhancement was defined as flat perinodular enhancement on late-phase CTAP images that was less than or equal to 2 mm thick. Type C nodules showed no portal perfusion, clearly increased arterial perfusion compared with background liver, and thick corona enhancement on late-phase CTHA images. Thick corona enhancement was defined as perinodular enhancement with or without irregular protrusions that was greater than 2 mm thick. We set this 2-mm threshold because we clinically observed that smooth or flat corona enhancement was exclusively less than 2 mm thick, and in contrast, irregular or protruding corona enhancement was almost always more than 2 mm thick.

Type A nodules corresponded to DNs or well-differentiated HCCs, and type B and C nodules were part of well-differentiated HCCs or, mainly, moderately differentiated HCCs (11–17). There was no case that showed apparent reduction of portal perfusion of the liver on CTAP images. Typical CTAP and CTHA findings for the three types of nodules are shown in Figure 1.

Pathologic Examinations

Liver specimens were fixed with neutral formalin, and 4-mm-thick paraffin-embedded tissue slices were prepared from each nodule. Hematoxylin-eosin staining was performed. To clearly differentiate each vessel, double immuno-

Figure 2

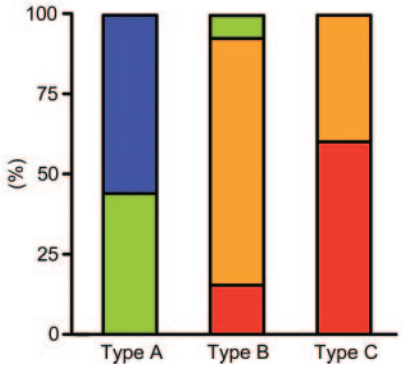

Figure 2: Bar graph of percentage of each tumor differentiation grade by tumor type. Blue = DN ($n = 10$), green = well-differentiated HCC ($n = 9$), orange = moderately differentiated HCC without fibrous capsule ($n = 16$), red = moderately differentiated HCC with fibrous capsule ($n = 11$).

Figure 3

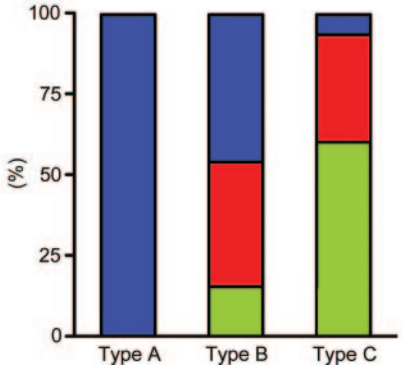

Figure 3: Bar graph of percentage of each histologic growth pattern by tumor type. Blue = replacing growth, red = compressing growth without fibrous capsule, green = compressing growth with fibrous capsule.

Figure 4

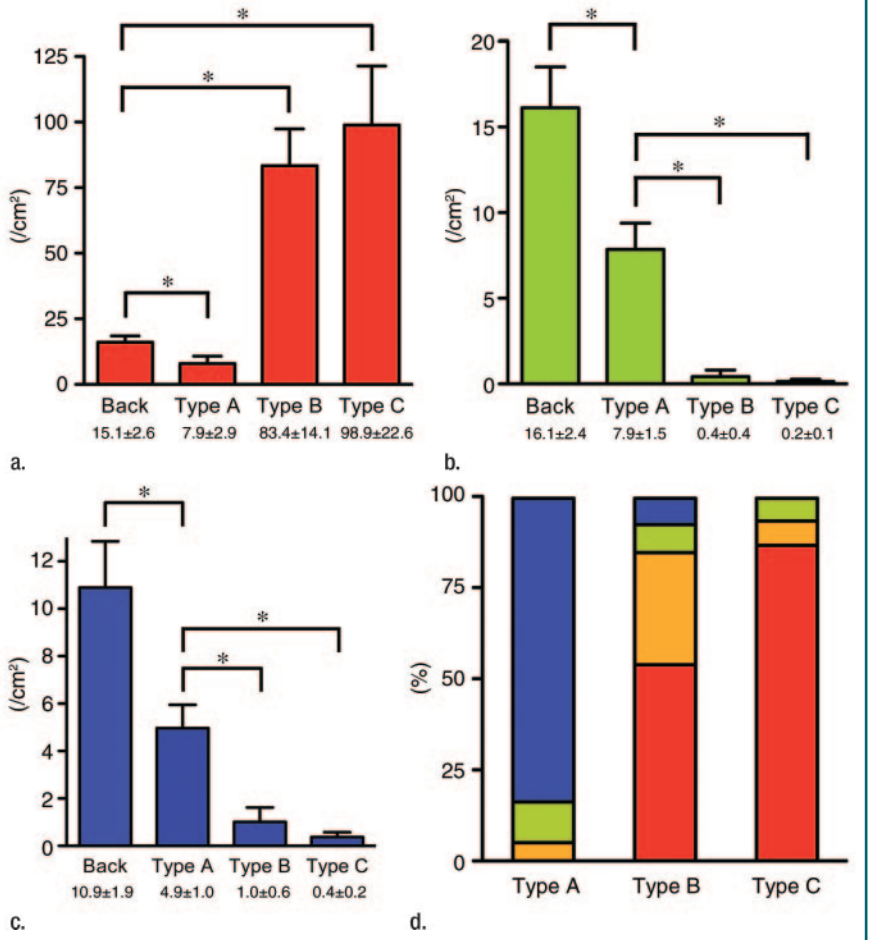

Figure 4: Bar graphs of density of intranodular vessels by nodule type compared with that in the background liver tissue *(Back)* for **(a)** arteries, **(b)** portal vein, and **(c)** hepatic vein. Mean value ± standard deviation is given under each bar. * = $P < .05$ with multiple comparison test. **(d)** Bar graph of percentage of area of capillarized sinusoids by nodule type shows progressive increase in percentage of capillarized area in type A versus type B versus type C nodules ($P < .05$ with Kruskal-Wallis test). Blue = 1+, green = 2+, orange = 3+, red = 4+.

Figure 5

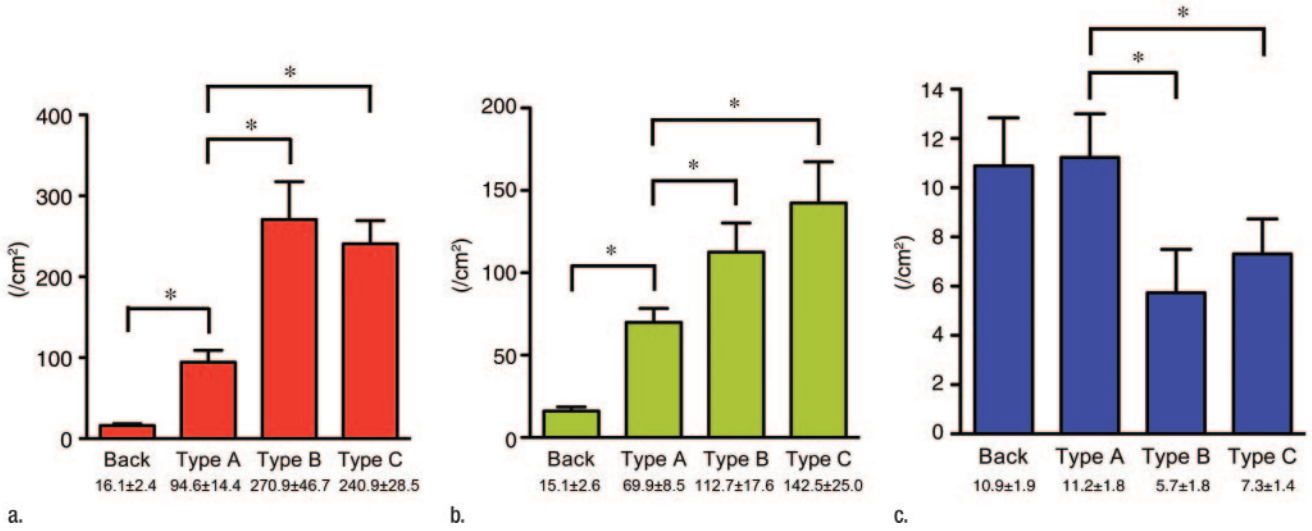

Figure 5: Bar graphs of density of perinodular vessels by nodule type compared with that in the background liver tissue *(Back)* for **(a)** arteries, **(b)** portal vein, and **(c)** hepatic vein. Mean value ± standard deviation is given under each bar. ∗ = $P < .05$ with **(a, b)** multiple comparison or **(c)** unpaired *t* test.

staining with CD34 (a vascular endothelial cell marker) and α–smooth muscle actin (a smooth muscle cell marker) was performed in all nodules. Two pathologists (Y.Z. and Y.N., with 11 and 37 years experience, respectively) and one radiologist (A.K.), who were blinded to all imaging information, evaluated the three nodule types in consensus for tumor differentiation, fibrous capsule formation, tumor growth pattern, background liver tissue (chronic hepatitis or liver cirrhosis), and number of vessels.

Tumor differentiation and fibrous capsule.—We classified each nodule into one of four grades for tumor differentiation according to the classifications proposed by the International Working Party (8) and the World Health Organization (23): DN, well-differentiated HCC, moderately differentiated HCC without fibrous capsule, and moderately differentiated HCC with fibrous capsule. A DN was defined as a small nodular lesion of hepatocytes with mild nuclear and cytoplasmic atypia, cellular density increase, and no evidence of malignancy (eg, stromal or vessel invasion). In our study, the DN category included both low- and high-grade DNs because they both show similar findings on CTAP and CTHA images (17). Well-differentiated HCC was de-

Figure 6

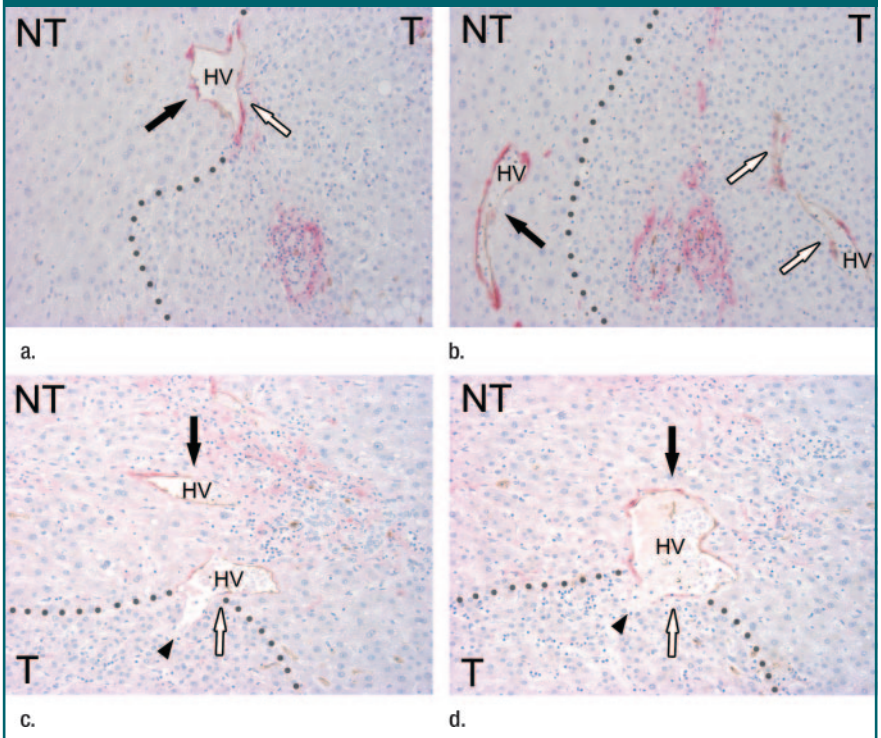

Figure 6: Serial pathologic slices show continuity of vessels at the border (dotted line) of a type A nodule (DN). **(a, b)** Intranodular preexisting hepatic vein (*HV,* white arrows) and extranodular hepatic veins (black arrows). **(c, d)** Intranodular capillarized sinusoid (arrowheads) continues into hepatic vein (white arrows) at nodule border and then into extranodular hepatic vein (black arrows). *NT* = not tumor, *T* = tumor. (Double immunostaining with CD34 [brown] and α–smooth muscle actin [red]; magnification, ×200.)

Figure 7

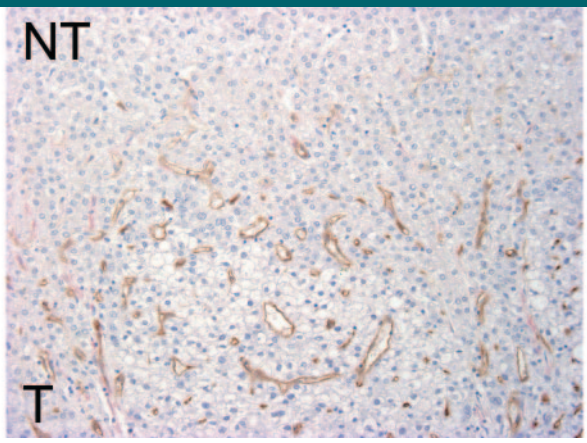

Figure 7: Continuities of intranodular capillarized sinusoids (brown) and extranodular hepatic sinusoids are diffusely observed at the border of a type B nodule (moderately differentiated HCC with replacing growth). *NT* = not tumor, *T* = tumor. (CD34 and α–smooth muscle actin; magnification, ×200.)

Figure 8

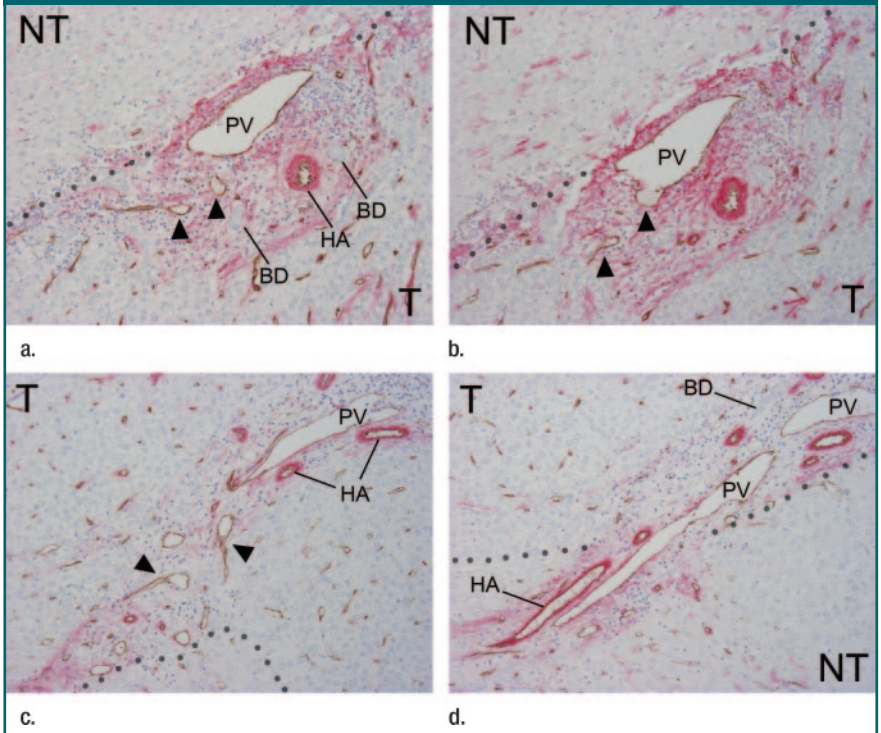

Figure 8: Continuities of vessels at border (dotted line) of a type C nodule (moderately differentiated HCC without fibrous capsule). Intranodular capillarized sinusoids (arrowheads) connect to extranodular portal veins *(PV)* **(a, b)** directly and **(c, d)** indirectly (through portal venules within the fibrous septum). Portal venules are accompanied by hepatic arteries *(HA)* and bile ducts *(BD)*. *NT* = not tumor, *T* = tumor. (CD34 and α–smooth muscle actin; magnification, ×200.)

fined as a nodular lesion consisting of malignant hepatocytes that showed evident nuclear and cytoplasmic atypia and higher cellular density. Intranodular portal tracts were relatively preserved. Moderately differentiated HCC was composed of malignant hepatocytes proliferating in trabecular, pseudoglandular, and solid patterns. We defined a fibrous capsule as fibrous tissue that was greater than 0.2 mm thick and surrounded more than two-thirds of the tumor circumference.

Tumor growth pattern.—Nodule growth patterns were classified into two types: replacing and compressing. In the nodules with replacing growth, tumor cells proliferated by replacing surrounding hepatic parenchyma, and the margin between nodules and background liver tissue was indistinct. Compressing-growth nodules had a discrete margin and pushed out the surrounding hepatic parenchyma.

Underlying disease process.—For each nodule type, we compared the proportion of patients with chronic hepatitis with that of patients with liver cirrhosis to analyze the influence of the underlying disease process on background liver tissue.

Number of vessels.—We counted the numbers of vessels twice. The number of arteries (both hepatic and neovascularized unpaired arteries), portal veins, and hepatic veins were counted in three areas: within tumor parenchyma, not including the fibrous septa or fibrous capsule; in the perinodular area less than 2 mm from the nodule border; and in the background liver away from the nodule. Intranodular and background liver vessels were counted in the largest square we could draw in the respective areas of the tissue slices. Perinodular vessels were counted in 10 random fields within 2 mm of the tumor border (magnification, ×100) or within as many fields as possible on small slices. Then, we divided the number of vessels by the area to calculate vessel density (per square centimeter).

We also measured the area of intranodular capillarized sinusoids covered by endothelial cells expressing CD34 and compared it with the whole

area of the nodule in the same slice (18,24). Capillarized area in each nodule was semiquantitatively rated as follows: 1+ = 0%–25%, 2+ = 26%–50%, 3+ = 51%–75%, and 4+ = 76%–100%.

Continuity of vessels at nodule border.—To clarify the continuity between intranodular vascular structures and extranodular drainage vessels at the border of the nodule, more than 200 serial slices were prepared from one tumor of each type (ie, A, B, and C). By using double immunostaining with CD34 and α–smooth muscle actin, we examined continuities between intranodular and extranodular vascular structures on serial slices.

Statistical Analysis

The data were expressed as means ± standard deviations. Statistical significance was evaluated by using the Kruskal-Wallis test for the comparison of tumor differentiation, tumor growth pattern, and the area of intranodular capillarized sinusoids; unpaired *t* test for the comparison of the number of perinodular hepatic veins between tumor types; and multiple comparison test (Dunnet procedure) for the analysis of the number of other vessels. *P* values less than .05 were considered to indicate statistical significance.

Results

Clinical Features by Nodule Type

Eighteen nodules were classified as type A; 13, as type B; and 15, as type C. The clinical features of the patients and the tumor sizes are listed by type in the Table. As determined from resected specimens, the mean size of all hepatocellular nodules was 2.4 cm ± 1.3.

Pathologic Features by Nodule Type

Tumor differentiation and fibrous capsule.—At histologic analysis (Fig 2), type A nodules consisted of 10 DNs and eight well-differentiated HCCs. Type B nodules comprised one well-differentiated HCC and 12 (92%) moderately differentiated HCCs, 10 (83%) of which did not have a fibrous capsule. All 15 type C nodules were moderately differentiated HCCs, nine (60%) of which had a fibrous capsule (Kruskal-Wallis test, $P < .05$).

Figure 9

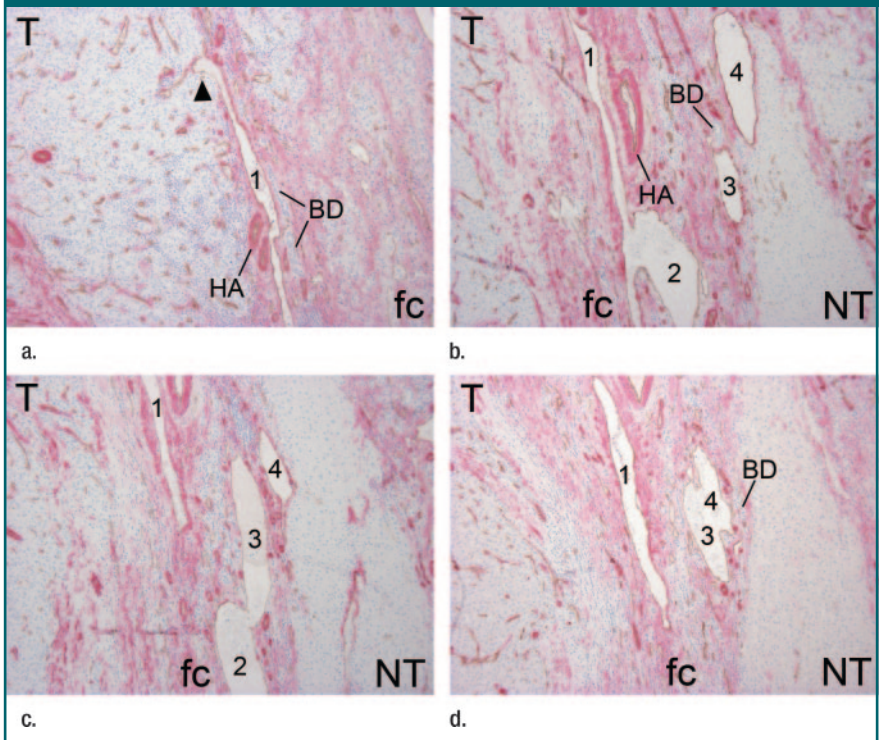

Figure 9: **(a–d)** Continuities of vessels at the border of a type C nodule (moderately differentiated HCC with fibrous capsule *[fc]*). Intranodular capillarized sinusoid (arrowhead, **a**) connects to portal venules (*1*, **a**) and drains into extranodular portal veins (*1–4*, **b–d**). *BD* = bile duct, *HA* = hepatic arteries, *NT* = not tumor, *T* = tumor. (CD34 and α–smooth muscle actin; magnification, ×100.)

Tumor growth pattern.—Histologic growth patterns for each type are shown in Figure 3. All of the type A nodules showed a replacing growth pattern. Half of type B nodules had replacing growth, and the other half had compressing growth. Almost all type C nodules (93%) showed compressing growth (Kruskal-Wallis test, $P < .05$). The proportion of nodules with compressing pattern was higher in type C than in type B (93% vs 54%).

Underlying disease process.—No significant difference with regard to histologic findings in the liver was observed between the three types of nodules. The percentages of chronic hepatitis and liver cirrhosis were 33% versus 67%, respectively, for type A nodules; 23% versus 77%, respectively, for type B nodules; and 33% versus 67%, respectively, for type C nodules.

Intranodular vessels.—Compared with the that in the background liver, the density of intranodular arteries was decreased in type A nodules and increased in type B and C nodules (all $P < .05$) (Fig 4). There was no statistically significant difference in the density of arteries between type B and C nodules. The density of intranodular portal veins was also decreased in type A nodules compared with the background liver and was decreased in type B and C nodules compared with type A nodules (all $P < .05$). The density of hepatic veins was similarly decreased ($P < .05$). The percentage of the nodule occupied by intranodular capillarized sinusoids progressively increased in type A versus B versus C nodules (Fig 4).

Perinodular vessels.—As shown in Figure 5, the density of perinodular arteries and portal veins was increased in type A nodules compared with the back-

ground liver ($P < .05$ with the multiple comparison test). In addition, type B and C nodules had higher densities of arteries and portal veins than did type A nodules ($P < .05$ with the multiple comparison test). In contrast, the density of hepatic veins around type B and C nodules was decreased compared with type A nodules ($P < .05$ with unpaired t test). No significant difference was observed in the density of any perinodular vessels between type B and type C nodules ($P < .05$).

Continuity of vessels at nodule border.—In the type A nodule, which was a DN, serial pathologic slices revealed the continuity between intranodular preexisting hepatic veins and extranodular hepatic veins (Fig 6a, 6b). In addition, intranodular capillarized sinusoids continued into extranodular hepatic veins (Fig 6c, 6d).

We also examined the serial pathologic slices of a type B nodule, which was a moderately differentiated HCC without a fibrous capsule that had a replacing growth pattern, for continuity of intranodular capillarized sinusoids and surrounding hepatic sinusoids (Fig 7). Intranodular and perinodular hepatic veins were rarely observed; therefore, their continuity was not confirmed.

We used two type C moderately differentiated HCCs to examine the continuity of vessels at the tumor border. One demonstrated compressing growth without a fibrous capsule, and the other showed compressing growth with a fibrous capsule. We observed many portal venules within the intranodular fibrous septa and the fibrous capsule, accompanied by hepatic arteries and bile ducts. In the nodule without a fibrous capsule, intranodular capillarized sinusoids connected to extranodular portal veins directly (Fig 8a, 8b). In addition, intranodular capillarized sinusoids connected to portal venules within the fibrous septum, and these portal venules continued into extranodular portal veins (Fig 8c, 8d). In the nodule with a fibrous capsule, intranodular capillarized sinusoids connected to portal venules within the fibrous capsule, with these venules connecting to extranodular portal veins (Fig 9).

Figure 10

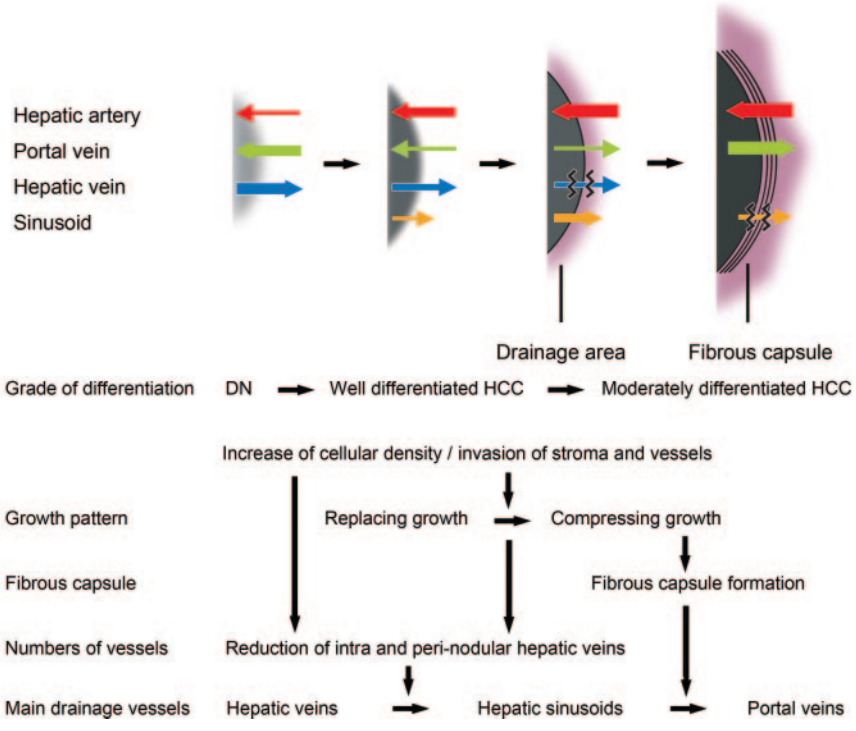

Figure 10: Diagram of the mechanism underlying changes in drainage vessels (top) and histologic features (bottom) of HCC during multistep hepatocarcinogenesis. Top: Direction of arrow = direction of flow for that vessel type. Thickness of arrow = volume through that vessel. Wavy lines through arrow = disruption of flow. Gray area = nodule.

Discussion

The different radiologic appearances of type A, B, and C nodules seem to be the direct result of several histologic features: the grade of tumor differentiation, fibrous capsule formation, and tumor growth pattern. According to the theory of multistep hepatocarcinogenesis, we think that these histologic features change as the nodules progress from type A (DN or well-differentiated HCC) to type B to type C (both moderately differentiated HCC). The results of our study suggest that the main drainage vessels change from hepatic veins (type A) to hepatic sinusoids (type B) and then to portal veins (type C) during this progression.

On the basis of our findings, a mechanism for how the drainage vessels of HCC change during multistep hepatocarcinogenesis can be postulated (Fig 10). As the tumor cells become more atypical and proliferate more rapidly, they first invade the intranodular hepatic veins because they are not accompanied by fibrous tissue (eg, Glisson's sheath surrounding portal veins). In the perinodular area, hepatic veins are similarly collapsed by tumor compression. Therefore, intranodular and perinodular hepatic veins disappear earlier than do portal veins. When the drainage through hepatic veins is blocked, drainage flows mainly into surrounding hepatic sinusoids and partially into portal veins according to the blood pressure gradient. As the intranodular cellular density increases, the tumor growth pattern changes from replacing growth to compressing growth, and a thick fibrous capsule is formed by the compressed perinodular liver tissue (25). At this stage, perinodular hepatic sinusoids are collapsed, and the conti-

nuity of intranodular and extranodular sinusoids is interrupted by fibrous capsule formation. Therefore, drainage blood flow has no outlet other than through portal veins, accompanied by a marked increase in arterial blood supply. Although the total number of intranodular portal veins is decreased, portal venules are relatively well preserved in the fibrous septa and capsule. These patent portal venules could become the drainage vessels of an established encapsulated HCC.

The direction of hepatic arterial flow is afferent, while that of hepatic venous flow is efferent owing to the pressure gradient. In contrast, the direction of portal flow to nodules is variable and can be determined by using the combination of CTAP and histologic findings. Type C nodules showed no portal perfusion at CTAP, and direct connections between intranodular capillarized sinusoids and portal venules were confirmed with histologic findings. We believe that the direction of portal flow would be efferent in type C nodules. That is, blood flow in portal veins seems to dramatically change during multistep hepatocarcinogenesis from afferent flow in type A nodules to efferent flow in type C nodules.

Previously, perinodular contrast enhancement was thought to represent the presence of a fibrous capsule (26,27). However, as shown in type C nodules, corona enhancement was frequently broader than the histologically confirmed fibrous capsule and included a protruding portion. Moreover, corona enhancement was also seen in nonencapsulated type B and C HCC nodules. Therefore, we conclude that corona enhancement consists of staining of mainly the perinodular parenchyma, although it might contain staining of the fibrous capsule, as well. However, the drainage area of type B nodules was thinner and smoother than that of type C nodules. This difference might be explained by the fact that the draining blood pressure or speed through surrounding hepatic sinusoids (type B nodules) might be lower than that through portal veins (type C nodules). Drainage area of type A nodules could not be observed because contrast material drained directly into the hepatic vein and did not pass through perinodular hepatic sinusoids. The corona enhancement findings at late-phase CTHA are surmised to closely correlate with the histologic changes of drainage vessels.

As has been previously reported (11–17), pathologic changes of arteries and portal veins in DNs and HCC are closely correlated with the radiologic findings. We should keep in mind that the background liver previous studies and ours used as the control does not represent normal liver (mainly chronic liver disease). In comparison to background liver, type A nodules had decreased intranodular arteries, and types B and C had significantly increased intranodular arteries and capillarized sinusoids. The findings on early-phase CTHA images reflected the histologic findings. In contrast, the density of intranodular portal veins decreased from type A to type B and C nodules, which corresponds to the findings on CTAP images.

In addition, we found an interesting pathologic feature; similar to intranodular portal veins, the density of intranodular hepatic veins markedly decreased from type A to type B and C nodules. Density of perinodular hepatic veins was also decreased in type B and C nodules, probably owing to tumor compression, whereas the densities of perinodular portal veins and hepatic arteries were increased. As mentioned above, hepatic veins might more readily collapse than would portal veins because of the absence of perivascular connective tissue. This impairment of blood flow through the hepatic veins could possibly trigger the dramatic change of drainage blood flow into the portal veins.

On the basis of the radiologic findings of our study, particularly corona enhancement, imaging can be used to provide insight into the grade of malignancy or drainage vessels of hepatocellular nodules. Drainage vessels seem to be a main factor in determining tumor progression, therefore understanding the drainage routes of HCC has implications for interventional therapy (eg, transarterial chemoembolization or ablation) and surgical resection (18,28). At transarterial chemoembolization of hypervascular HCCs, outflow of iodized oil into perinodular portal veins or surrounding parenchyma is often observed (29,30). This finding suggests that the drainage vessels are portal veins or sinusoids. Nodule drainage has been shown to influence the treatment efficacy of transarterial chemoembolization (31).

Our study had several limitations. First, serial slices of only four nodules were used to evaluate the continuity of vessels at the nodule border. In the remaining nodules the drainage route was surmised from the number of vessels in the tumor and surrounding liver in correlation with the CTAP and CTHA findings. Second, quantitative analysis of all drainage vessels was not feasible. Therefore, in the case of mixed drainage routes (eg, portal veins and surrounding hepatic sinusoids), the main route could not be accurately determined. However, we do not believe these factors negate the new concept proposed in our study.

In conclusion, the main drainage vessels of hepatocellular nodules change from hepatic veins to surrounding hepatic sinusoids and then to portal veins during multistep hepatocarcinogenesis. This change seems to be triggered by the early disappearance of intranodular and perinodular hepatic veins. This notion is important for understanding pathophysiologic and radiologic features of DN, early HCC, and moderately differentiated HCC.

References

1. Villa E, Baldini GM, Pasquinelli C, et al. Risk factors for hepatocellular carcinoma in Italy: male sex, hepatitis B virus, non-A non-B infection, and alcohol. Cancer 1988;62:611–615.

2. Unoura M, Kaneko S, Matsushita E, et al. High-risk groups and screening strategies for early detection of hepatocellular carcinoma in patients with chronic liver disease. Hepatogastroenterology 1993;40:305–310.

3. Takayama T, Makuuchi M, Hirohashi S, et al. Malignant transformation of adenomatous hyperplasia to hepatocellular carcinoma. Lancet 1990;336:1150–1153.

4. Sakamoto M, Hirohashi S, Shimosato Y. Early stages of multistep hepatocarcinogenesis: adenomatous hyperplasia and early hepatocellular carcinoma. Hum Pathol 1991;22:172–178.
5. Kobayashi M, Ikeda K, Hosaka T, et al. Dysplastic nodules frequently develop into hepatocellular carcinoma in patients with chronic viral hepatitis and cirrhosis. Cancer 2006; 106:636–647.
6. Nakanuma Y, Terada T, Terasaki S, et al. Atypical adenomatous hyperplasia in liver cirrhosis: low-grade hepatocellular carcinoma or borderline lesion? Histopathology 1990;17:27–35.
7. Nakanuma Y, Terada T, Ueda K, Terasaki S, Nonomura A, Matsui O. Adenomatous hyperplasia of the liver as a precancerous lesion. Liver 1993;13:1–9.
8. Terminology of nodular hepatocellular lesions: International Working Party. Hepatology 1995;22:983–993.
9. Nakashima O, Sugihara S, Kage M, Kojiro M. Pathomorphologic characteristics of small hepatocellular carcinoma: a special reference to small hepatocellular carcinoma with indistinct margins. Hepatology 1995; 22:101–105.
10. Nakano M, Saito A, Yamamoto M, Doi M, Takasaki K. Stromal and blood vessel wall invasion in well-differentiated hepatocellular carcinoma. Liver 1997;17:41–46.
11. Matsui O, Kadoya M, Kameyama T, et al. Benign and malignant nodules in cirrhotic livers: distinction based on blood supply. Radiology 1991;178:493–497.
12. Hayashi M, Matsui O, Ueda K, Kawamori Y, Gabata T, Kadoya M. Progression to hypervascular hepatocellular carcinoma: correlation with intranodular blood supply evaluated with CT during intraarterial injection of contrast material. Radiology 2002;225:143–149.
13. Matsui O, Takashima T, Kadoya M, et al. Dynamic computed tomography during arterial portography: the most sensitive examination for small hepatocellular carcinomas. J Comput Assist Tomogr 1985;9:19–24.
14. Takayasu K, Muramatsu Y, Furukawa H, et al. Early hepatocellular carcinoma: appearance at CT during arterial portography and CT arteriography with pathologic correlation. Radiology 1995;194:101–105.
15. Murakami T, Takamura M, Kim T, et al. Double phase CT during hepatic arteriography for diagnosis of hepatocellular carcinoma. Eur J Radiol 2005;54:246–252.
16. Tajima T, Honda H, Taguchi K, et al. Sequential hemodynamic change in hepatocellular carcinoma and dysplastic nodules: CT angiography and pathologic correlation. AJR Am J Roentgenol 2002;178:885–897.
17. Hayashi M, Matsui O, Ueda K, et al. Correlation between the blood supply and grade of malignancy of hepatocellular nodules associated with liver cirrhosis: evaluation by CT during intraarterial injection of contrast medium. AJR Am J Roentgenol 1999;172:969–976.
18. Park YN, Yang CP, Fernandez GJ, Cubukcu O, Thung SN, Theise ND. Neoangiogenesis and sinusoidal "capillarization" in dysplastic nodules of the liver. Am J Surg Pathol 1998; 22:656–662.
19. Ueda K, Terada T, Nakanuma Y, Matsui O. Vascular supply in adenomatous hyperplasia of the liver and hepatocellular carcinoma: a morphometric study. Hum Pathol 1992;23: 619–626.
20. Toyosaka A, Okamoto E, Mitsunobu M, Oriyama T, Nakao N, Miura K. Intrahepatic metastases in hepatocellular carcinoma: evidence for spread via the portal vein as an efferent vessel. Am J Gastroenterol 1996;91: 1610–1615.
21. Tochio H, Kudo M. Afferent and efferent vessels of premalignant and overt hepatocellular carcinoma: observation by color Doppler imaging. Intervirology 2004;47:144–153.
22. Ueda K, Matsui O, Kawamori Y, et al. Hypervascular hepatocellular carcinoma: evaluation of hemodynamics with dynamic CT during hepatic arteriography. Radiology 1998;206:161–166.
23. Hirohashi S, Ishak KG, Kojiro M, et al. Hepatocellular carcinoma. In: Hamilton SR, Aaltonen LA, eds. Pathology and genetics of tumours of the digestive system. Lyon, France: IARC, 2000; 157–172.
24. Nakamura K, Zen Y, Sato Y, et al. Vascular endothelial growth factor, its receptor Flk-1, and hypoxia inducible factor-1alpha are involved in malignant transformation in dysplastic nodules of the liver. Hum Pathol 2007;38:1532–1546.
25. Okuda K, Musha H, Nakajima Y, et al. Clinicopathologic features of encapsulated hepatocellular carcinoma: a study of 26 cases. Cancer 1977;40:1240–1245.
26. Ros PR, Murphy BJ, Buck JL, Olmedilla G, Goodman Z. Encapsulated hepatocellular carcinoma: radiologic findings and pathologic correlation. Gastrointest Radiol 1990; 15:233–237.
27. Lim JH, Choi D, Park CK, Lee WJ, Lim HK. Encapsulated hepatocellular carcinoma: CT-pathologic correlations. Eur Radiol 2006;16: 2326–2333.
28. Sakon M, Nagano H, Nakamori S, et al. Intrahepatic recurrence of hepatocellular carcinoma after hepatectomy. Arch Surg 2002; 137:94–99.
29. Matsui O, Kadoya M, Yoshikawa J, et al. Small hepatocellular carcinoma: treatment with subsegmental transcatheter arterial embolization. Radiology 1993;188:79–83.
30. Terayama N, Matsui O, Gabata T, et al. Accumulation of iodized oil within the nonneoplastic liver adjacent to hepatocellular carcinoma via the drainage routes of the tumor after transcatheter arterial embolization. Cardiovasc Intervent Radiol 2001;24:383–387.
31. Miyayama S, Matsui O, Yamashiro M, et al. Ultraselective transcatheter arterial chemoembolization with a 2-f tip microcatheter for small hepatocellular carcinomas: relationship between local tumor recurrence and visualization of the portal vein with iodized oil. J Vasc Interv Radiol 2007;18:365–376.